International Journal of Mechanical Engineering and Smart Technology
ISSN: xxxx-xxxx (Print) | ISSN: xxxx-xxxx (Online)

Vol. 01, No. 1 (2026) | Page 01–17 | DOI: 10.XXXXX/ijomest.XXXX.XXXX | Received: 13 May 2026 · Accepted: 25 My 2026

Thermal Effects on Drying Performance, Kinetics, and Quality Characteristics of Paddy

M. Yahya[1], Zido Yuwazama[2]*, Dedi Wardianto[3], Arfidian Rachman[4], Ismet Eka Putra[5], Putra Andi Kolala[6]

[1] *Department of Mechanical Engineering, Faculty of Engineering, Institut Teknologi Padang, Padang, Indonesia*
[2] *Department of Mechanical Engineering, Faculty of Engineering, Institut Teknologi Padang, Padang, Indonesia*
[3] *Department of Mechanical Engineering, Faculty of Engineering, Institut Teknologi Padang, Padang, Indonesia*
[4] *Department of Mechanical Engineering, Faculty of Engineering, Institut Teknologi Padang, Padang, Indonesia*
[5] *Department of Mechanical Engineering, Faculty of Engineering, Institut Teknologi Padang, Padang, Indonesia*
[6] *Department of Mechanical Engineering, Faculty of Industrial Technology, Institut Teknologi Sumatera, South Lampung, Indonesia*

**Corresponding author:* Zido Yuwazama, zidoyuwazama23@gmail.com

A B S T R A C T

A solar hybrid continuous dryer (SHCD) was developed to overcome the limitations of conventional solar batch drying systems for paddy. This study investigates the thermal effects on drying performance, drying kinetics, and quality characteristics of paddy at different drying air temperatures. Drying experiments were conducted at average air temperatures of 49.7 °C (Exp 1), 60.0 °C (Exp 2), and 69.6 °C (Exp 3). The results indicate that the SHCD at an air temperature drying of 60.0 °C provides the optimal balance between drying performance, energy efficiency, and product quality. At this temperature, the drying time was significantly reduced, accompanied by higher thermal efficiency and superior rice quality compared to other conditions. In contrast, drying at 49.7 °C resulted in prolonged drying time, whereas drying at 69.6 °C led to reduced thermal efficiency and deterioration in product quality. Moreover, the SHCD at 60.0 °C reduced the paddy mass from 420 kg (16.80% wet basis) to 407.63 kg (14.17% wet basis) within 165.4 min. The average drying rate, specific moisture extraction rate (SMER), and specific energy consumption (SEC) were 2.849 kg/h, 0.125 kg/kWh, and 15.649 kWh/kg, respectively, with a maximum thermal efficiency of 17.14%. Quality analysis showed that the percentages of head rice, broken rice, and rice groats were 85.60 ± 0.65%, 8.73 ± 1.98%, and 4.92 ± 1.67%, respectively. Furthermore, the drying kinetics analysis revealed that the moisture ratio (MR) data were best described by the Page model, indicating its suitability for predicting paddy drying behavior in the SHCD system. These findings present that temperature optimization plays a critical role in enhancing drying efficiency and maintaining product quality in continuous solar drying systems.

K E Y W O R D S Paddy; drying; kinetic; quality; performance

1. INTRODUCTION

Indonesia, as an agriculture-based country, is recognized as one of the world's leading paddy producers. In 2019, national paddy production reached approximately 84 million tons, with an annual per capita rice consumption of about 111.58 kg, indicating that rice remains a staple food with consistently high demand [1]. Due to the tropical climate characterized by high humidity, freshly harvested paddy must be dried immediately to prevent mold growth, discoloration, and quality deterioration. Typically, harvested paddy contains a moisture content ranging from 20% to 27% wet basis (wb), which must be reduced to approximately 14% wet basis (wb) to ensure safe storage and extend shelf life [2].

© 2026 IJOMEST · Published under CC BY 4.0 License

Traditionally, paddy drying is carried out using open sun drying, where grains are directly exposed to solar radiation. This method is widely practiced due to its advantages, including the availability of free and abundant solar energy, operational simplicity, and low initial and maintenance costs. However, open sun drying also has limitations, especially the requirement of large drying areas, dependence on weather conditions, prolonged drying time, susceptibility to contamination, pest infestation, and material losses. Moreover, this method often results in non-uniform drying and product quality reduction [3].

To address these limitations, mechanical drying technologies, including flat-bed dryers, have been developed and extensively implemented. These systems provide enhanced drying efficiency, reduced drying time, improved control over operating conditions, and minimized material losses during the drying process [4]. Flat-bed dryers continue to encounter significant challenges, particularly in achieving uniform temperature and moisture distribution within the grain bed. In practice, drying non-uniformity commonly occurs between the upper and lower layers of the paddy bed. The upper layer tends to retain higher moisture content due to insufficient heat transfer, while the lower layer becomes excessively dry due to prolonged exposure to heated air.

This non-uniformity significantly affects rice quality during milling. Tahrir reported that, in a 50 cm thick paddy bed dried using a flat-bed dryer, the percentage of broken rice was 7.35% in the upper layer and 13.80% in the lower layer. These values exceed the maximum allowable limit specified in SNI 6128:2008 (5%) [5]. The high percentage of broken rice is mainly attributed to uneven moisture distribution, which induces internal stresses within the grain, leading to fissures and breakage during milling.

Drying temperature is one of the most critical parameters affecting drying performance, energy consumption, and rice quality. Previous studies have demonstrated that excessive drying temperatures can significantly degrade grain quality. Astuti reported that drying at 95 °C resulted in an extremely high broken rice percentage of 87.5% after milling [6]. Similarly, Karbasi and Mehdizadeh found that drying at 140 °C reduced head rice yield and negatively affected the sensory properties of rice, including taste and aroma [7]. Furthermore, Yahya et al. reported that drying using a recirculating mixed-flow dryer at temperatures of 75.40 °C – 81.40 °C resulted in moderate head rice yield (67.37% ± 0.69%) and relatively high broken rice (26.34% ± 0.80%), indicating quality degradation at elevated temperatures [8].

The deterioration in rice quality at high drying temperatures is primarily caused by rapid moisture removal, which creates steep moisture gradients within the grain. This leads to internal stress, fissure formation, and structural damage in the endosperm, making the grains more prone to breakage during milling. Additionally, excessive heat exposure can alter rice's physicochemical properties, leading to undesirable changes in flavor and aroma. Therefore, precise control of drying temperature and uniform heat distribution are crucial to maintain both the physical and sensory quality of rice.

Recent advancements in drying technology have introduced hybrid drying systems that integrate renewable energy sources with advanced control mechanisms. Yahya et al. evaluated a hybrid solar-assisted heat pump dryer and reported significant improvements in both drying performance and product quality. The system achieved efficient moisture reduction within 5.5 hours at an average temperature of 62.9 °C, with a high head rice yield (93.10% ± 1.044%) and low broken rice (4.41% ± 0.737%). These results highlight the potential of hybrid drying systems to provide controlled drying conditions, improved energy efficiency, and more uniform moisture removal [9].

Despite these advancements, studies on solar hybrid continuous drying systems remain limited, particularly in terms of comprehensive evaluation involving thermal performance, drying kinetics, and product quality under different temperature conditions. Most existing studies focus on either drying performance or product quality separately, leaving a research gap in the integrated analysis of these parameters.

Therefore, this study aims to investigate the thermal effects on drying performance, drying kinetics, and quality characteristics of paddy using a solar hybrid continuous dryer (SHCD). Drying experiments were conducted at various air temperatures to evaluate key performance indicators, including drying rate, specific energy consumption, and thermal efficiency. In addition, drying kinetics were evaluated using established mathematical models, while product quality was assessed based on milling characteristics. The findings of this study are expected to provide valuable insights into optimizing operating conditions for continuous solar drying systems and improving the overall quality of dried paddy.

© 2026 IJOMEST · Published under CC BY 4.0 License

2. METHODOLOGY

a. Experimental Set-up

A solar hybrid continuous dryer (SHCD) for paddy consists of a blower, bucket elevator, drying column, biomass furnace, and vibratory feeder. The biomass furnace includes a heat exchanger, blower, chimney, and combustion chamber. The construction of the biomass furnace employed AISI 1030 steel plates, SK-34 cement mortar, and SK-34 fire bricks due to their superior mechanical strength and high-temperature resistance, whereas the heat exchanger pipes were manufactured from mild steel. The drying column comprises three essential units: the discharge, the drying, and the storage. The discharge system consists of a motor-driven mechanical assembly, while the vibratory feeder and bucket elevator facilitate continuous material handling. A cross-sectional area of 95 × 95 cm² in the drying section incorporates outlet and inlet air ducts arranged in a horizontal configuration. Each side consists of four rows of ducts, with six inlet ducts per row and a combination of five full and two half outlet ducts per row. Each duct has a cross-sectional area of 56.25 cm² and a wedge-shaped design to enhance airflow distribution. Photographs and schematic diagrams of the SHCD and its components are presented in Figures 1–6.

Figure 1. The solar hybrid continuous dryer (SHCD).

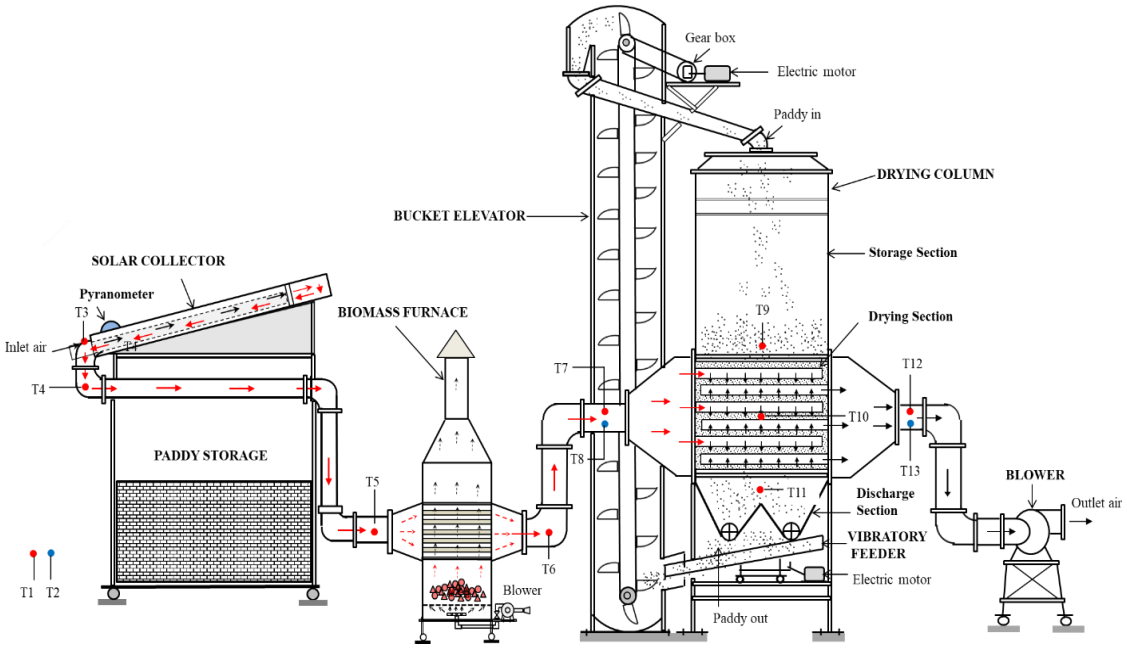

Figure 2. Schematic of the SHCD.

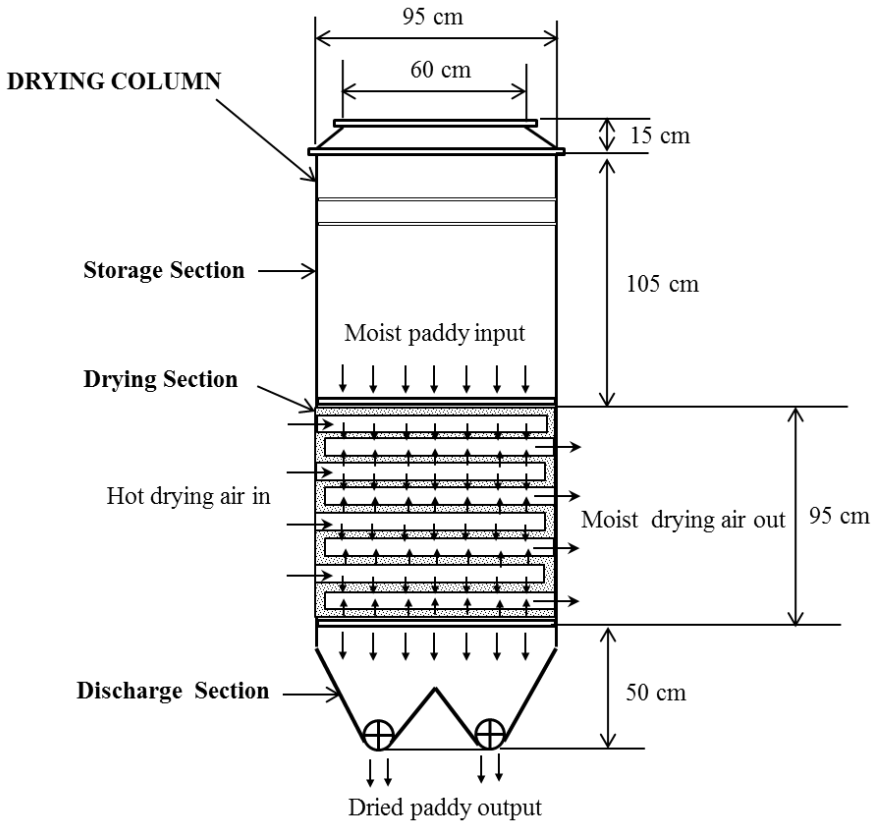

Figure 3. Schematic of the drying column with dimensions.

Figure 4. The air duct.

© 2026 IJOMEST · Published under CC BY 4.0 License

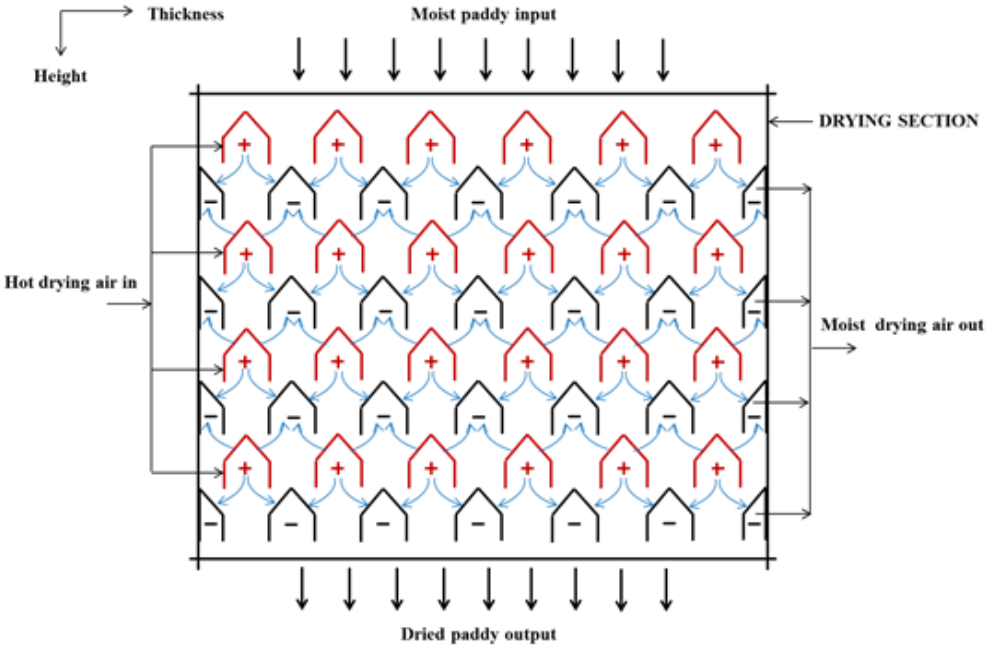

Figure 5. Air duct configuration in drying section with hot air inlet (+) and moist air outlet (-).

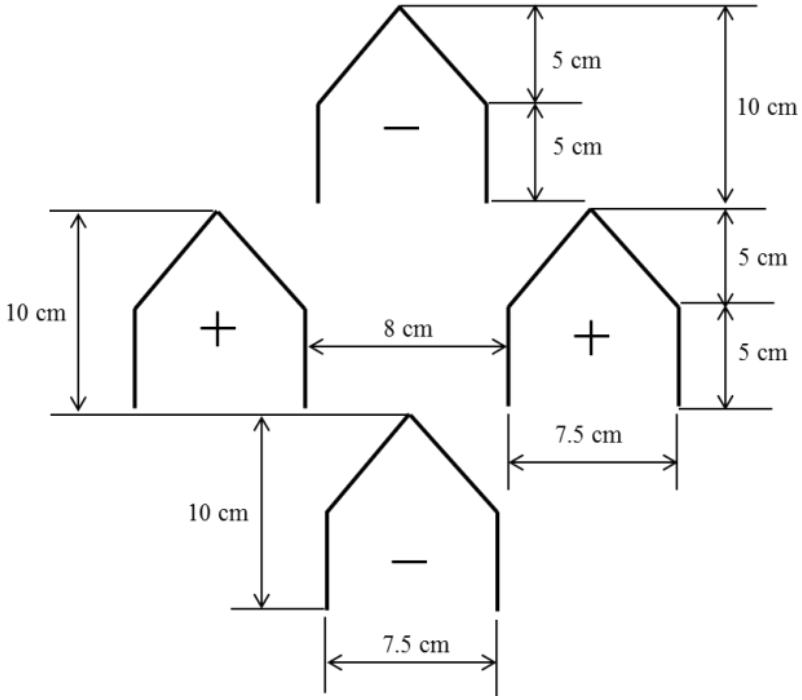

Figure 6. Dimensions of the air ducts.

b. Experimental Procedure

Drying tests were carried out to analyze the performance of the SHCD system with a 420 kg capacity. Local farmers provided fresh paddy for this experiment. In the experiment, type-T thermocouples (± 0.1°C) were employed to measure ambient temperature, air temperature, and paddy temperature at the SHCD system. Air velocity at the inlet and outlet of the drying section was measured using an anemometer (± 0.2 m/s). All temperature data were recorded using a data logger (± 0.1°C). The paddy moisture content was determined using a digital grain moisture tester (± 0.5%), while the masses of biomass fuel (coconut shell charcoal) and paddy were measured using digital weighing scales (±0.05 kg and ±0.1 kg, respectively). All parameters were recorded at 30-minute intervals. Measurement uncertainty was calculated using the following equation [10, 11]:

$$W_R = \left[\left(\frac{\partial R}{\partial x_1} w_1\right)^2 + \left(\frac{\partial R}{\partial x_2} w_2\right)^2 + \cdots + \left(\frac{\partial R}{\partial x_n} w_n\right)^2\right]^{-\frac{1}{2}} \quad (1)$$

© 2026 IJOMEST · Published under CC BY 4.0 License

where WR is the total uncertainty in the result measurement; the corresponding uncertainties in the aforementioned independent variables are w1, w2, ..., wn. While the independent variables are x1, x2, ..., xn.

c. Analysis of Drying Kinetics and Performance

Drying kinetics were evaluated in terms of moisture content, drying rate, and dimensionless moisture ratio (MR). The goodness of fit of the drying models was assessed using the root-mean-square error (RMSE), mean bias error (MBE), and coefficient of determination (R^2). The SHCD performance was analyzed based on key parameters, including drying rate ($\dot{m}_{water}$), specific moisture evaporation rate (SMER), specific energy consumption (SEC), thermal efficiency of the dryer (η_{th}), and biomass furnace efficiency (η_{BF}). All drying kinetics and performance parameters were calculated using the equations listed in Table 1.

Table 1. Equations used to determine the drying kinetic and performance of the SHCD.

Parameter	Formula	Eq.	Ref.
Drying kinetic			
Paddy moisture content (wb)	$M_{wbpd} = \frac{m_{wetpd} - m_{dpd}}{m_{wetpd}}$	(2)	[12]
Moisture content of paddy (db)	$M_{dbpd} = \frac{m_{wetpd} - m_{dpd}}{m_{dpd}}$	(3)	[12]
Drying rate (DR)	$\dot{m}_{water} = \frac{M_{dbpd,t+dt} - M_{dbpd,t}}{dt}$	(4)	[13, 14]
Dimensionless moisture content	$MR = \frac{M_t}{M_o}$	(5)	[11, 15]
Newton model	$MR = \exp(-kt)$	(6)	[11, 15]
Henderson and Pabis model	$MR = a \exp(-kt)$	(7)	[11, 15]
The root-mean-square error	$RMSE = \left[\frac{1}{N}\sum_{i=1}^{N}(MR_{pre,i} - MR_{exp,i})^2\right]^{\frac{1}{2}}$	(8)	[11, 15]
The mean bias error	$MBE = \frac{1}{N}\sum_{i=1}^{N}(MR_{pre,i} - MR_{exp,i})^2$	(9)	[11, 15]
Page model	$MR = \exp(-kt^n)$	(10)	[11, 15]
Performance of dryer			
Specific energy consumption	$SEC = \frac{Q_{Ise} + Q_{Ibmf} + W_C + W_{Bd} + W_{Bbf} + W_{Mt}}{\dot{m}_{water}}$	(11)	[16,17]
Total electrical energy input of electrical motor	$W_{Mt} = W_{Mbe} + W_{Mvf} + W_{Mdr}$	(12)	[16,17]
Specific moisture extraction rate	$SMER = \frac{\dot{m}_{water}}{Q_{Ise} + Q_{Ibmf} + W_C + W_{Bd} + W_{Bbf} + W_{Mt}}$	(13)	[17,18]
Thermal dryer efficiency	$\eta_{th} = \frac{m_{water} H_{fg}}{Q_{Ise} + Q_{Ibmf} + W_C + W_{Bd} + W_{Bbf} + W_{Mt}}$	(14)	[19,20]
Drying system component's performance			

© 2026 IJOMEST · Published under CC BY 4.0 License

Collector efficiency	$\eta_{SC} = \frac{Q_{EPsc}}{Q_{Ise}} \times 100\%$	(15)	[19,21]
Biomass furnace efficiency	$\eta_{BF} = \frac{Q_{EPbf}}{Q_{Ibmf}} \times 100\%$	(16)	[22]
Thermal energy input of solar collector	$Q_{Ise} = I_T A_{SC}$	(17)	[19, 21]
Power input of compressor	$W_C = VI \cos \varphi$	(18)	[19,23]
Power input of dryer blower	$W_{Bfd} = \sqrt{3} VI \cos \varphi$	(19)	[23]
Thermal energy input of biomass furnace	$Q_{Ibmf} = \dot{m}_{bf} C_{Pda}$	(20)	[22]
Thermal energy produced by solar collector	$Q_{EPsc} = \dot{m}_a C_a (T_{o,sc} - T_{i,sc})$	(21)	[21]
Thermal energy produced by biomass furnace	$Q_{EPbf} = \dot{m}_a C_a (T_{o,bf} - T_{i,bf})$	(22)	[22]

d. Quality of Drying Products

Beyond drying performance and drying time, the quality of the dried product is a critical parameter that must be considered. Product quality is strongly influenced by drying air temperature, as excessive temperatures may result in quality degradation. In paddy drying, product quality is commonly evaluated based on milling outcomes, including the percentages of head rice yield, broken rice, and rice groats. These parameters were determined following the milling of the dried paddy. The corresponding percentages of rice groats, broken rice, and head rice yield obtained from the SHCD system were calculated using the equations presented in Table 2.

Table 2. Equations used to determine the quality of drying product.

Parameter	Equation	Eq.no.	Ref.
Head rice yield	$HRY = \frac{W_{THR}}{W_{TS}} \times 100\%$	(23)	[24]
Broken rice	$BR = \frac{W_{TBR}}{W_{TS}} \times 100\%$	(24)	[25]
Grain grouts	$GG = \frac{W_{TGG}}{W_{TS}} \times 100\%$	(25)	[26]

3. RESULTS AND DISCUSSION

The uncertainties related to the experimental parameters in paddy drying are summarized in Table 3.

Table 3. Uncertainty evaluation of experimental parameters in paddy drying.

Parameter	Unit	Range of Uncertainty
Paddy temperature	°C	± 0.20
Air temperature	°C	± 0.20
Time measurement	min	± 0.10
Paddy moisture content change	% (wb)	± 0.51
Relative humidity	%	± 0.35
Mass of paddy	kg	± 0.14

© 2026 IJOMEST · Published under CC BY 4.0 License

Mass of coconut shell charcoal	kg	± 0.11
Air velocity	m/s	± 0.24

The variation of solar radiation with drying time at different drying temperatures is presented in Figure 7. During experiments (Exp 1, 2, and 3), the weather conditions were generally clear. For an average air temperature of 49.7 °C (Exp. 1), solar radiation ranged from 365.94 W/m² to 796.51 W/m², with an average value of 592.47 W/m². At 60.0 °C (Exp. 2), solar radiation varied between 469.09 W/m² and 766.55 W/m², with an average of 643.28 W/m². Similarly, at 69.6 °C (Exp. 3), solar radiation ranged from 402.32 W/m² to 923.62 W/m², with an average value of 630.63 W/m².

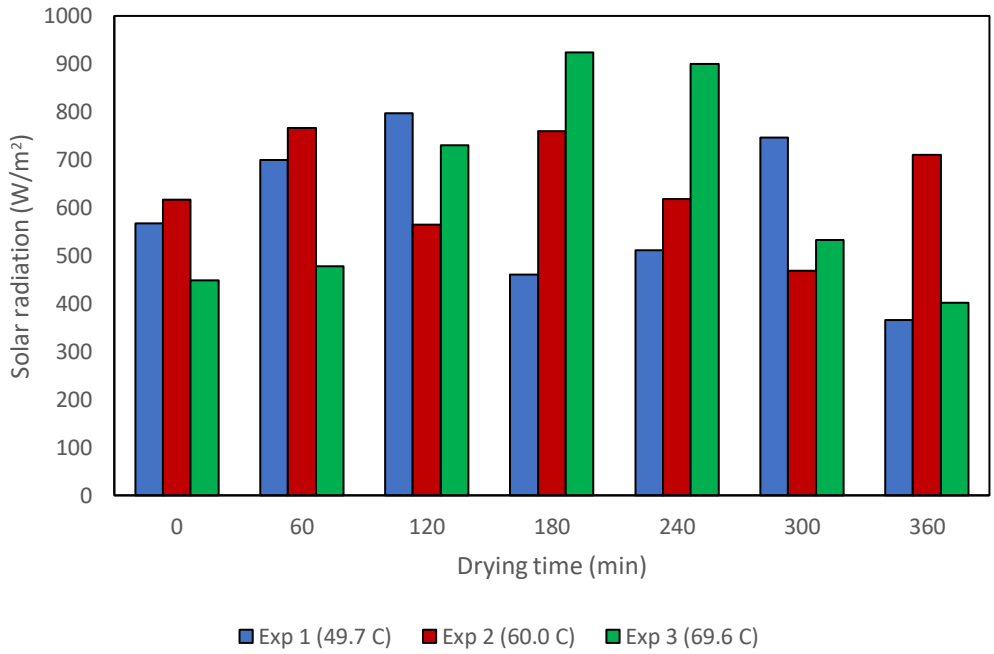

Figure 7. Variation of solar radiation with drying time.

The variation of solar collector efficiency with drying time at different drying temperatures is presented in Figure 8. For an average air temperature of 49.7 °C (Exp. 1), the solar collector efficiency ranged from 62.86 % to 97.06 %, with an average value of 82.15%. At 60.0 °C (Exp. 2), the efficiency varied between 67.46 % and 88.53 %, with an average of 79.46%. Meanwhile, at 69.6 °C (Exp. 3), the efficiency ranged from 55.60 % to 80.70 %, with an average value of 70.67%. The results indicate that the highest average solar collector efficiency was achieved at the lower drying temperature (49.7 °C). This is mainly due to the smaller temperature difference between the collector and ambient air, which reduces thermal losses. At higher drying temperatures (69.6 °C), efficiency declines as a result of greater heat dissipation to the environment and diminished heat transfer performance. Although the efficiency at 60.0 °C is slightly lower than that at 49.7 °C, it provides a better balance between energy utilization and drying performance, as reflected in the shorter drying time and improved overall system performance.

© 2026 IJOMEST · Published under CC BY 4.0 License

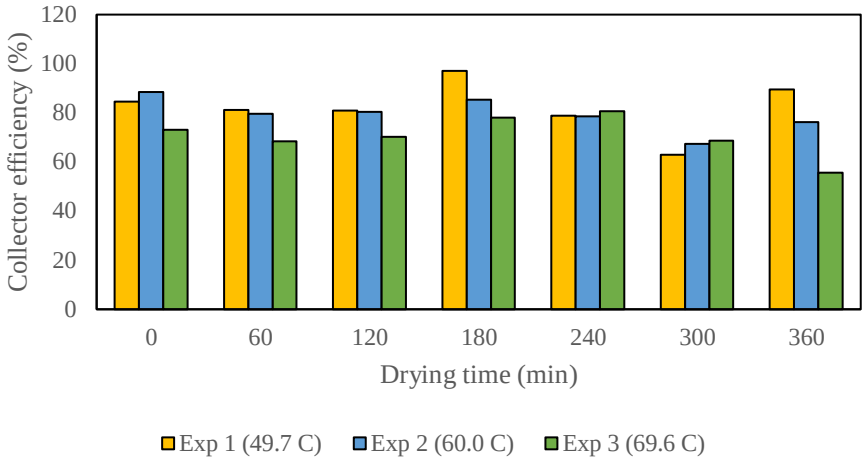

Figure 8. Changes in solar collector efficiency over drying time.

Figure 9 illustrates the variation of biomass furnace thermal efficiency with drying time at various drying temperatures. The thermal efficiency of biomass furnace ranged from 20.26 % to 38.20 %, 21.45 % to 27.21 %, and 22.79 % to 32.46 % for air temperatures of 49.7 °C (Exp. 1), 60.0 °C (Exp. 2), and 69.6 °C (Exp. 3), respectively. The corresponding average efficiencies were 29.14 %, 24.55 %, and 27.04 %. The results show that the highest average thermal efficiency was obtained at 49.7 °C, while the lowest occurred at 60.0 °C. This behavior can be attributed to the variation in heat demand and combustion conditions within the biomass furnace. At lower drying temperatures, the heat requirement is relatively moderate, allowing more stable combustion and improved heat utilization. In contrast, at higher drying temperatures, increased fuel consumption and heat losses reduce the overall efficiency. Although the efficiency at 60.0 °C is lower than that at 49.7 °C, this condition provides more effective heat utilization for the drying process, as indicated by improved drying performance and shorter drying time. This suggests that optimal dryer operation not only depends on furnace efficiency but also involves balancing heat supply and drying requirements.

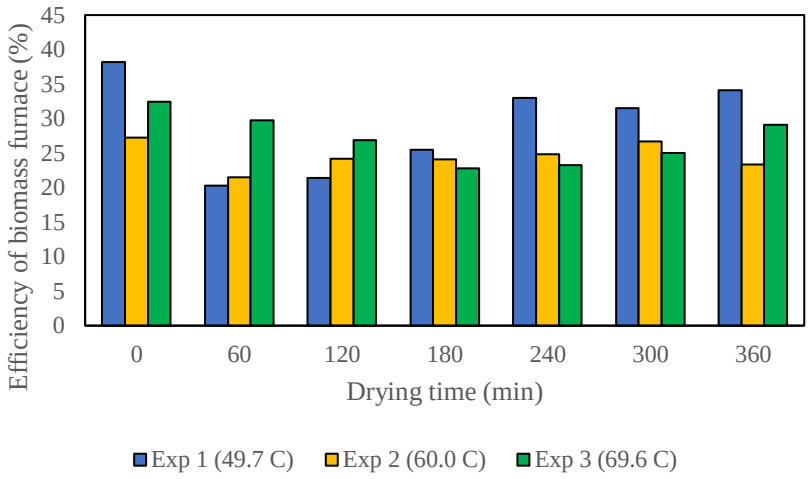

Figure 9. Effect of drying time on biomass furnace efficiency.

The relationship between drying air temperature and drying time at various operating conditions is presented in Figure 10. The drying air temperatures for Experiments 1–3 ranged from 49.30 to 50.80 °C, 58.20 to 61.40 °C, and 68.50 to 70.40 °C, respectively, with average values of 49.7 °C, 60.0 °C, and 69.6 °C. The results indicate that the drying system was able to maintain relatively stable air temperatures throughout the drying process, with only minor fluctuations observed in each experiment. This stability reflects the effective integration of the solar collector and biomass furnace in providing a consistent heat supply. Furthermore, the controlled temperature ranges demonstrate that the SHCD system can operate reliably under different thermal conditions, enabling a systematic evaluation of temperature effects on drying performance, kinetics, and product quality. The small temperature variations also ensure that the observed differences in drying behavior are primarily influenced by the set operating temperatures rather than thermal instability within the system.

© 2026 IJOMEST · Published under CC BY 4.0 License

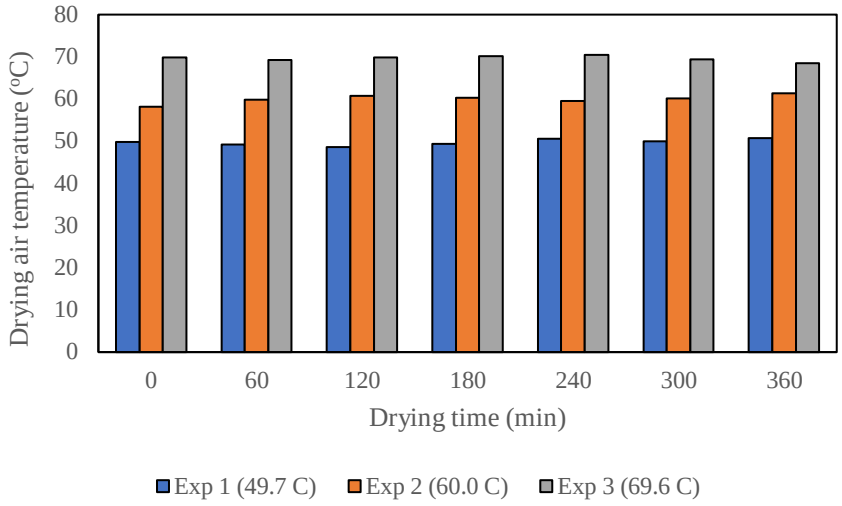

Figure 10. The relationship between drying air temperature and drying time.

Figure 11 illustrates the change in paddy moisture content over drying time under a variation in drying air temperatures. As anticipated, the moisture content decreases progressively with drying time under all temperature conditions, with higher temperatures resulting in significantly faster moisture removal rates. At an average drying air temperature of 49.7 °C (Exp. 1), the moisture content decreased in the range 16.90% wb to 14.17% wb, corresponding to a reduction in paddy mass from 420 kg to 406.07 kg over a drying period of 360 min. In comparison, at an average drying air temperature of 60.0 °C (Exp. 2), the system achieved the same final moisture content of 14.17% wb in a much shorter time of 165.43 min, with the final mass recorded at 407.63 kg. Furthermore, for the highest drying air temperature of 69.6 °C (Exp. 3), the drying process was further accelerated, reaching the target moisture content of 14.17% wb within 143.29 min, with a final mass of 407.35 kg. These results clearly indicate that increasing the drying air temperature enhances the drying kinetics, thereby reducing the drying time required to reach the desired moisture content. This behavior can be attributed to the higher thermal energy supplied at elevated temperatures, which increases the vapor pressure gradient between the surrounding air and the paddy surface, thereby promoting faster moisture diffusion and evaporation. However, while higher temperatures improve drying efficiency, careful consideration is required to avoid potential quality degradation of the paddy.

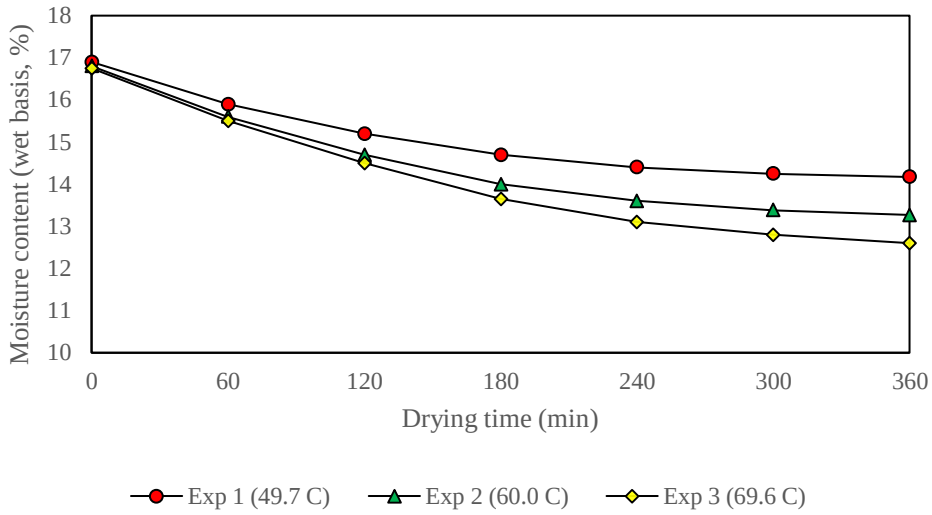

Figure 11. Paddy moisture content (wb) as a function of drying time.

The variation in drying rate over drying time in experiment is presented in Figure 12. In general, the drying rate exhibits a decreasing trend with drying time for all temperature conditions, indicating that the drying process is predominantly governed by the falling-rate period. The drying rates obtained from the solar hybrid continuous dryer at average air temperatures of 49.7 °C (Exp 1), 60.0 °C (Exp 2), and 69.6 °C (Exp 3) show a clear dependence on temperature. At an average air temperature of 49.7 °C, the drying rate ranged from 0.379 to 4.994 kg/h, with an average value of 2.226 kg/h. An increase in drying air temperature to 60.0 °C resulted in an enhanced drying rate,

© 2026 IJOMEST · Published under CC BY 4.0 License

varying between 0.512 and 5.972 kg/h, with an average value of 2.849 kg/h. A further increase in temperature to 69.6 °C resulted in the highest drying performance, with drying rates ranging from 0.918 to 6.213 kg/h and an average value of 3.324 kg/h. The higher drying rates observed at elevated temperatures can be attributed to the increased heat transfer to the paddy, which enhances moisture evaporation from the surface as well as internal moisture diffusion. Initially, the drying rate is relatively high due to the abundance of free moisture on the surface. However, as drying progresses, the rate gradually decreases because moisture migration becomes controlled by internal diffusion mechanisms. These findings demonstrate that increasing the drying air temperature significantly enhances the drying kinetics and overall system performance. Nevertheless, excessive temperatures should be carefully controlled to prevent potential thermal damage and maintain the quality of the dried paddy.

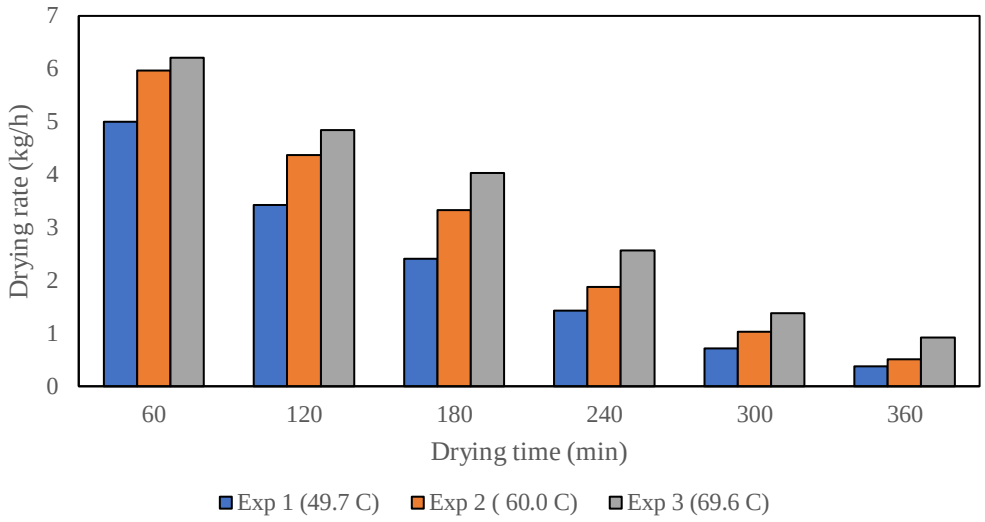

Figure 12. The relationship between drying rate and drying time.

The relationship between specific moisture extraction rate (SMER) and drying time at different drying temperatures is presented in Figure 13. At air temperatures of 49.7 °C, 60.0 °C, and 69.6 °C, the SMER ranged between 0.032–0.378 kg/kWh, 0.022–0.259 kg/kWh, and 0.034–0.227 kg/kWh, respectively, with corresponding mean values of 0.171, 0.125, and 0.118 kg/kWh. Figure 13 also illustrates the variation of specific energy consumption (SEC) with drying time under the same conditions. At drying temperatures of 49.7 °C, 60.0 °C, and 69.6 °C, the SEC varied between 2.643–31.631 kWh/kg, 3.860–44.652 kWh/kg, and 4.402–29.512 kWh/kg, respectively, with corresponding mean values of 11.804 kWh/kg, 15.649 kWh/kg, and 13.018 kWh/kg. The results indicate that SMER tends to decrease with increasing drying temperature, suggesting a reduction in energy utilization efficiency at higher temperatures. This behavior is attributed to increased heat losses and reduced effectiveness of moisture removal per unit energy input. Conversely, SEC shows an increasing trend with temperature, particularly at 60.0 °C, indicating higher energy consumption per unit mass of evaporated moisture. Although the highest SMER was obtained at 49.7 °C, this condition is associated with longer drying time. In contrast, drying at 60.0 °C provides a more favorable trade-off between energy consumption and drying efficiency, resulting in improved overall system performance. These findings highlight that optimal drying operation requires a balance between energy efficiency and drying effectiveness, rather than maximizing a single parameter

© 2026 IJOMEST · Published under CC BY 4.0 License

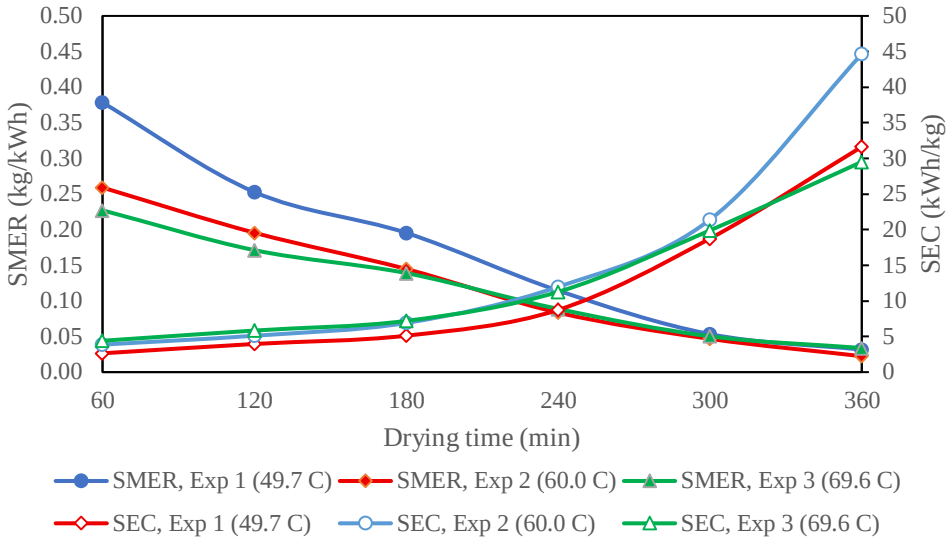

Figure 13. SMER and SEC trends during the drying process.

The relationship between the thermal efficiency of the dryer and drying time at different drying air temperatures is illustrated in Figure 14. In general, the thermal efficiency fluctuates throughout the drying process, reflecting variations in heat utilization and moisture removal rates over time. The thermal efficiency of the dryer for average air temperatures of 49.7 °C (Exp. 1), 60.0 °C (Exp. 2), and 69.6 °C (Exp. 3) was found to be in the ranges of 2.09–25.04%, 1.48–17.14%, and 2.24–15.03%, respectively. The corresponding average thermal efficiencies were 11.32%, 8.30%, and 7.83%. It can be observed that the highest average thermal efficiency was achieved at the lowest drying air temperature (49.7 °C). This behavior indicates that, although higher temperatures accelerate the drying rate, they do not necessarily lead to better thermal efficiency. At elevated temperatures, a significant portion of the supplied thermal energy may be lost to the surroundings or carried away by the exhaust air, thereby reducing the effective utilization of heat for moisture evaporation. Moreover, at lower drying temperatures, the heat supplied to the system is utilized more effectively for moisture removal, resulting in higher thermal efficiency. The decrease in thermal efficiency with increasing temperature suggests a trade-off between drying rate and energy efficiency, which is a critical consideration in the design and optimization of solar hybrid drying systems. These findings highlight the importance of selecting an optimal drying temperature that balances drying time, energy consumption, and product quality to achieve an efficient and sustainable drying process.

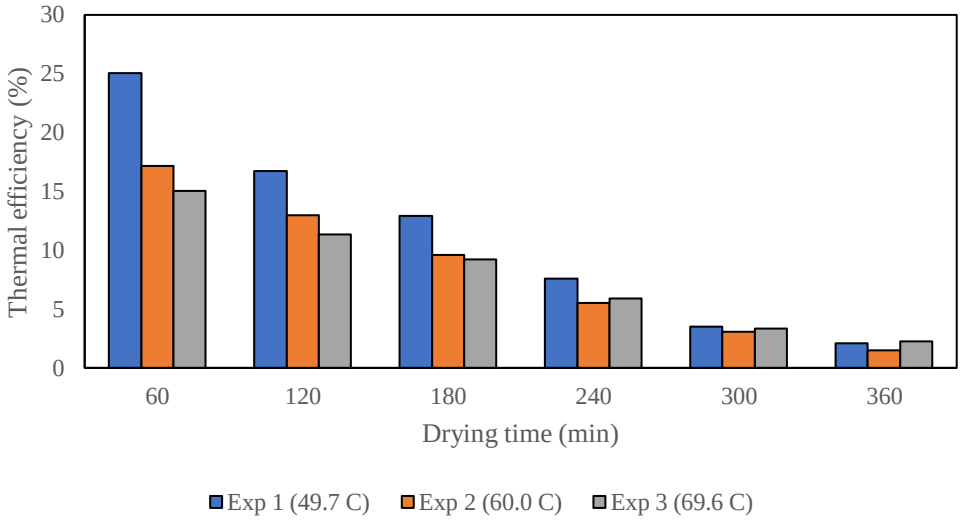

Figure 14. The relationship between thermal efficiency and drying time.

Three thin-layer drying models, namely Page, Henderson–Pabis, and Newton models, were employed to fit the dimensionless moisture content data of dried paddy at various drying air temperatures. The regression constants, along with the statistical indicators including root mean square error (RMSE), mean bias error (MBE), the coefficient of determination (R^2), are presented in Table 4. The Page model provided the best fit to the experimental. This is

© 2026 IJOMEST · Published under CC BY 4.0 License

evidenced by its higher R^2 values and lower MBE and RMSE values, indicating better agreement between the predicted and experimental results. Through an average air temperature of 49.7 °C for paddy drying, the Page model yielded R^2 = 0.9645, MBE = 0.00007, and RMSE = 0.00847. At an average air temperature of 60.0 °C, the model performance improved slightly, with R^2 = 0.9673, MBE = 0.00013, and RMSE = 0.01127. Furthermore, at the highest drying air temperature of 69.6 °C, the Page model demonstrated the best overall performance, with R^2 = 0.9784, MBE = 0.00014, and RMSE = 0.01178. These results confirm that the Page model is appropriate for characterizing the drying behavior of paddy in the solar hybrid continuous dryer within the investigated temperature range. The superior performance of the Page model can be attributed to its empirical flexibility, which allows it to better capture the nonlinear moisture removal characteristics during the falling-rate drying period. Figure 15 presents a comparison between the experimental MR and the MR predicted by the Page model for the dryer. The results confirm the suitability of the developed model in representing the drying behavior of paddy.

Table 4. Drying kinetics and statistical evaluation of thin-layer models for paddy drying.

Model	Temp.	Coefficients			R^2	MBE	RMSE
		a	k	n			
Newton	50		0.036		0.9001	0.00061	0.02460
	60		0.047		0.9200	0.00079	0.02827
	70		0.055		0.9496	0.00066	0.02579
Henderson and Pabis	50	1.0308	0.0286		0.8942	0.00397	0.06308
	60	1.0357	0.0390		0.9126	0.00506	0.07111
	70	1.0322	0.0478		0.9434	0.00398	0.06307
Page	50		0.6027	0.0659	0.9645	0.00007	0.00847
	60		0.6597	0.0802	0.9673	0.00013	0.01127
	70		0.7414	0.0830	0.9784	0.00014	0.01178

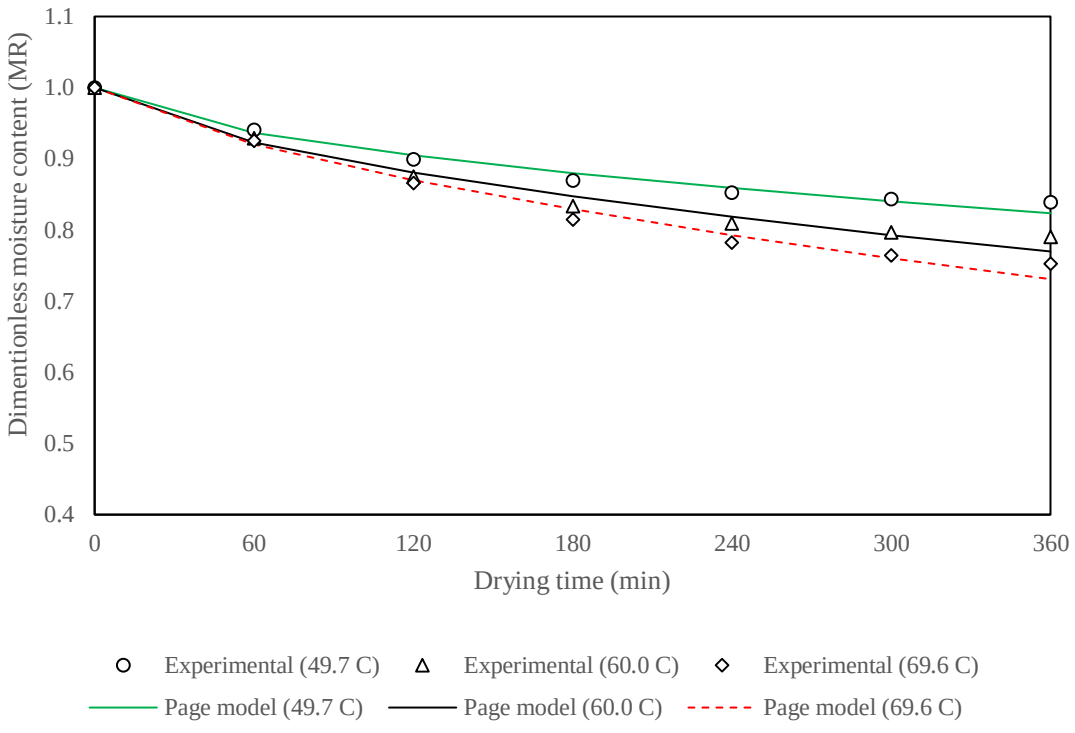

Figure 15. The relationship between dimensionless moisture content (MR) and drying time.

© 2026 IJOMEST · Published under CC BY 4.0 License

The variation in rice quality components as a function of drying air temperature is presented in Figure 16. Milled rice quality was assessed based on the distribution of head rice, broken rice, and rice groats after processing the dried paddy. For the drying air temperature range of 49.30–50.80 °C, with an average temperature of 49.7 °C, the percentages of head rice, broken rice, and rice groats were 88.41 ± 1.46%, 7.14 ± 0.48%, and 3.01 ± 0.72%, respectively. When the drying air temperature increased to the range of 58.20–61.40 °C (average 60.0 °C), the head rice yield decreased to 85.60 ± 0.65%, while the proportions of broken rice and rice groats increased to 8.73 ± 1.98% and 4.92 ± 1.67%, respectively. A more pronounced effect was observed at the highest drying air temperature range of 68.50–70.40 °C (average 69.6 °C), where the head rice percentage significantly decreased to 72.85 ± 4.54%, accompanied by a substantial increase in broken rice (14.14 ± 2.50%) and rice groats (7.85 ± 1.46%). These results clearly indicate that increasing the drying air temperature adversely affects the milling quality of rice. Higher temperatures tend to induce internal stresses and fissures within the rice kernels due to rapid moisture removal and uneven moisture gradients. As a result, the grains become more susceptible to breakage during the milling process, leading to a reduction in head rice yield and an increase in broken fractions. Therefore, although higher drying temperatures can significantly reduce drying time, they negatively impact the final product quality. This highlights the importance of optimizing the drying temperature to achieve a balance between drying efficiency and rice quality, particularly in solar hybrid continuous drying systems. The experimental results of paddy drying using the SHCD system are summarized in Table 5.

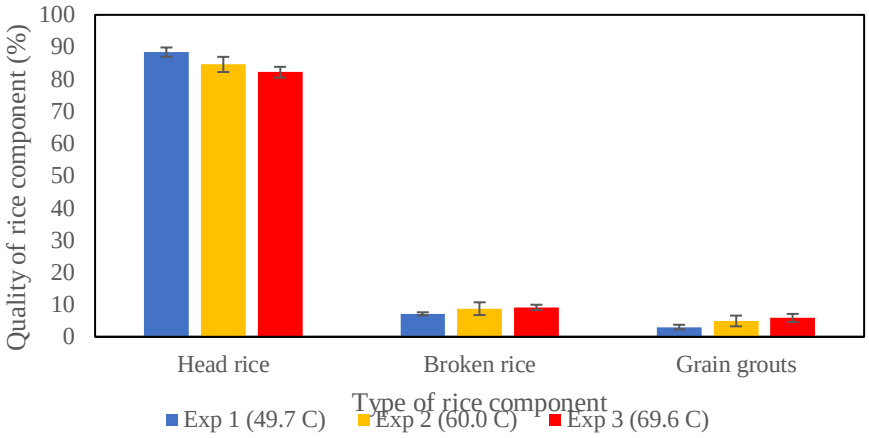

Figure 16. The relationship between quality of rice component and type of rice component.

Table 5. Evaluation of the performance of SHCD and the quality of drying products.

Parameter	Unit	Value		
		Exp 1	Exp 2	Exp 3
Initial weight of paddy	kg	420	420	420
Final weight of paddy	kg	406.6	407.6	407.3
Initial moisture content (wb)	%	16.90	16.80	16.75
Final moisture content (wb)	%	14.17	14.17	14.17
Average drying air temperature	°C	49.7	60.0	69.6
Drying time	min	360	165.4	143.3
Average drying rate	kg/h	2.226	2.849	3.324
Average SMER	kg/kWh	0.171	0.125	0.118
Average SEC	kWh/kg	11.80	15.65	13.02
Average thermal efficiency of the SHCD	%	11.32	8.30	7.83
Average efficiency of solar collector	%	82.2	79.5	70.7

© 2026 IJOMEST · Published under CC BY 4.0 License

Average efficiency of biomass furnace	%	29.1	24.6	27.0
Head rice yield	%	88.41±1.456	85.60±0.651	72.85±4.541
Broken rice	%	7.14±0.475	8.73±1.983	14.14±2.500
Grain grouts	%	3.01±0.723	4.92±1.670	7.85±1.455

4. CONCLUSION

This study aimed to design, construct, and evaluate the performance of a solar hybrid continuous dryer (SHCD) for paddy drying. The following conclusions are drawn from the experimental outcomes:

1. A combination of solar energy and biomass fuel effectively met the thermal energy demand of the drying process, confirming the system's hybrid performance.
2. The average solar collector efficiencies were 82.15%, 79.46%, and 70.67% at average drying air temperatures of 49.7 °C (Exp. 1), 60.0 °C (Exp. 2), and 69.6 °C (Exp. 3), indicating a decreasing trend with increasing temperature.
3. The biomass furnace efficiencies were 29.14% (Exp. 1), 24.55% (Exp. 2), and 27.04% (Exp. 3), and, respectively, showing relatively stable but moderate performance.
4. The drying system successfully reduced the moisture content of paddy from approximately 16.75–16.90% wb to 14.17% wb, with drying times significantly decreasing from 360 min to 143.3 min as the drying air temperature increased.
5. The average drying rates increased with temperature, reaching 2.226 kg/h, 2.849 kg/h, and 3.324 kg/h for Exp. 1, Exp. 2, and Exp. 3, respectively, confirming enhanced drying kinetics at higher temperatures.
6. In contrast, the average SMER values decreased from 0.171 kg/kWh to 0.118 kg/kWh with increasing temperature, while the SEC values varied between 11.804 kWh/kg and 15.649 kWh/kg, indicating a trade-off between drying rate and energy efficiency.
7. The maximum thermal efficiencies of the dryer were 25.04% (Exp. 1), 17.14% (Exp. 2), and 15.03% (Exp. 3), suggesting that lower drying temperatures resulted in more effective heat utilization.
8. The drying behavior of paddy was best described by the Page model, which showed the highest coefficient of determination and lowest error values among the evaluated models.
9. In terms of product quality, the highest head rice yield (88.41 ± 1.46%) was obtained at the lowest drying temperature (49.7 °C), while higher temperatures led to increased proportions of broken rice and groats, indicating quality degradation due to thermal stress and grain fissuring.

Overall, the SHCD system demonstrated effective performance for paddy drying, with a clear trade-off between drying rate, energy efficiency, and product quality. Therefore, an optimal drying air temperature in the moderate range (around 50–60 °C) is recommended to achieve a balance between drying efficiency and rice quality.

NOMENCLATURE

C_{Pa}	air specific heat (Jkg^{-1}C^{-1})
CV_{Bmf}	biomass fuel caloric value (kcal/kg)
$cos\ \varphi$	power factor
E_{Bbf}	electrical energy required by the biomass furnace blower (W)
E_{bmf}	heat energy produced from burning of the biomass fuel (W)
E_{Bmfd}	electrical energy required by the mixed flow dryer blower (W)
E_{Mbe}	electrical energy required by the bucket elevator motor (W)
E_{Mdr}	electrical energy required by the discharge roller motor (W)
E_{Mvf}	electrical energy required by the vibratory feeder motor (W)
H_{fg}	latent heat of vaporization of water (kJ/kg)
I	current (A)

© 2026 IJOMEST · Published under CC BY 4.0 License

$\dot{m}_a$	mass flow rate of air (kg/s)
$\dot{m}_{bmf}$	consumption rate of biomass fuel (kg/h)
$m_{bonedrypd}$	mass of bone dry of paddy (kg)
$M_{Cdb,t}$	paddy moisture content (dry basis) at the time "t"
$M_{Cdb,t+\Delta t}$	paddy moisture content (dry basis) at the time "$t+\Delta t$"
M_O	initial paddy moisture content (%)
M_t	instantaneous paddy moisture content (%)
$\dot{m}_{water}$	drying rate (kg/h)
$\dot{m}_{wetpd}$	mass of wet of paddy (kg)
T	temperature (°C)
V	voltage (V)
Δt	interval of drying time (h)

AUTHORS' CONTRIBUTIONS

MY contributed to the conceptualization of the study, methodology development, data curation, data validation, writing of the original draft, and project administration. **ZY** was responsible for investigation, formal analysis, writing the original draft, and reviewing and editing the manuscript. **DW** contributed to methodology development, data visualization, validation, and project administration. **AR** was responsible for formal analysis, supervision, manuscript review and editing, and project administration. **IP** contributed to formal analysis, data visualization, data curation, and validation. **PK** contributed to formal analysis, manuscript review and editing, data visualization, and data curation.

REFERENCES

[1] BPS (Badan Pusat Statistik Indonesia), "Statistik Indonesia," Jakarta, 2019.

[2] Bonazzi, F. Courteis, C. Geneste, M. C. Lahon, & J. Bimbent, "Influence of drying conditions on the processing quality of rough rice," Drying Technology, vol. 51, no. 3, pp. 1141–1157, 1997.

[3] D. B. Brooker, F. W. Bakker–Arkema, & C. W. Hall, "Drying and storage of grains and oilseeds," New York: Van Nostrand Reinhold. 1992.

[4] D. C. Wang, & Y. C. Lee, "Performance evaluation of reversible air flow drying in circulating dryer," Int. Journal of Advances in Chemical Eng. & Biological Science, vol. 4, no. 1, pp. 185–190, 2017.

[5] R. Thahir, "Pengaruh aliran udara dan ketebalan pengeringan terhadap mutu gabah keringannya," Buletin Enjiniring Pertanian VII (1&2), 1–5. 2000.

[6] Astuti, "Pengeringan padi dalam unggun bergerak dua tahap". Institut Teknologi Bandung: Skripsi, 2007.

[7] A. Karbassi, & Z. Mehdizabeh. "Drying rough rice in a fluidized bed dryer". Journal of Agricultural Science and Technology, vol. 10, no. 3, pp. 233–241. 2008.

[8] M. Yahya, H. Fahmi, & H. Hasibuan, "Experimental performance analysis of a pilot-scale biomass-assisted recirculating mixed-flow dryer for drying paddy," International Journal of Food Science, pp. 1–15, 2022.

[9] M. Yahya, H. Fahmi, R. Hasibuan, & A. Fudholi, "Development of hybrid solar-assisted heat pump dryer for drying paddy," Case Studies in Thermal Engineering, vol. 45, 102936, 2023.

[10] E. K. Akpinar, "Drying of mint leaves in a solar dryer and under open sun: Modelling, performances analyses," Energy Conversion and Management, vol. 51, pp. 2407–2418, 2010.

[11] M. Yahya, H. Fahmi, A. Fudholi, & K. Sopian, "Performance and economic analyses on solar-assisted heat pump fluidised bed dryer integrated with biomass furnace for rice drying," Solar Energy, vol. 174, pp. 1058–1067, 2018.

[12] M. S. H. Sarker, M. N. Ibrahim, N. Ab. Aziz, & P. M. Salleh, "Energy and rice quality aspects during drying of freshly harvested paddy with industrial inclined bed dryer," Energy Conversion and Management, vol. 77, pp. 389–395, 2014.

© 2026 IJOMEST · Published under CC BY 4.0 License

[13] C. W. Cao, D.Y. Yang, & Q. Liu, “Research on modeling and simulation of mixed-flow grain dryer,” Drying Technology, vol. 25, pp. 681–687, 2007.

[14] J. Prasad, & V.K. Vijay, “Experimental studies on drying of Zingiber officinale, Curcuma l. and Tinosopora cardifolia in solar-biomass hybrid dryer,” Renewable Energy, vol. 30, pp. 2097–2109, 2005.

[15] M. Yahya, “Design and performance evaluation of a solar assisted heat pump dryer integrated with biomass furnace for red chilli,” International Journal of Photoenergy, pp. 1–14, 2016.

[16] M. Yapa, “Design and testing of pilot continuous fluidized bed paddy dryer,” M.Eng thesis, King Mongkut’s University of Technology Thonburi, Bangkok, Thailand, 139, 1994.

[17] S. Soponronnarit, M. Yapha, & S. Prachayawarakorn, “Crossflow fluidized bed paddy dryer: prototype and commercialization,” Drying Technology, vol. 13, no. 8–9, pp. 2207–2216, 1995.

[18] M. C. Ndukwu, M. Simo-Tagne, F. I. Abam, O. S. Onwuka, & L. Bennamoun, “Exergetic sustainability and economic analysis of hybrid solar-biomass dryer integrated with copper tubing as heat exchanger,” Heliyon, vol. 6, no. 2, e03401, 2020.

[19] H. T. Jokiniemi, & J. M. Ahokas, “Drying process optimisation in a mixed-flow bacth grain dryer,” Biosystems Engineering, vol. 121, pp. 209–220, 2014.

[20] Y. M. Yunus, H. H. Al-Kayiem, & K. A. K. Albaharin, “Design of a biomass burner/gas-to-gas heat exchanger for thermal backup of a solar dryer,” Journal of Applied Sciences, vol. 11, no. 11, pp. 1929–1936, 2011.

[21] M. A. Billiris, & T. J. Siebenmorgen, “Energy use and efficiency of rice drying systems II. Commercial, cross-flow dryer measurements,” Applied Engineering in Agriculture, vol. 30, no. 2, pp. 217-226, 2014.

[22] W. Jittanit, N. Saeteaw, & A. Charoenchaisri, “Industrial paddy drying and energy saving options,” Journal of Stored Products Research, vol. 46, pp. 209–213, 2010.

[23] M. A. Leon, & S. Kumar, “Design and performance evaluation of a solar-assisted biomass drying system with thermal storage,” Drying Technology, vol. 26, pp. 936–947, 2008.

[24] M. N. Ibrahim, M. S. H. Sarker, N. Ab Aziz, & P. M. Salleh, “Drying performances and milling quality of rice during industrial fluidized bed drying of paddy in Malaysia,” Pertanika Journal of Science and Technology, vol. 23, no. 2, 297–309, 2015.

[25] R. J. Pontawe, R. C. Martinez, N. T. Asuncion, & R. B. Villacorte, “Development of a fully-automated pilot-scale model fluidized bed drying system for complete drying of paddy,” Asian Journal of Applied Sciences, vol. 3, no. 6, pp. 747–758, 2015.

[26] S. Mehran, M. Nikian, M. Ghazi, H. Zareiforoush, & I. Bagheri, “Experimental investigation and energy analysis of a solar-assisted fluidizedbed dryer including solar water heater and solar-powered infrared lamp for paddy grains drying,” Solar Energy, vol. 190, pp. 167–184, 2019.

© 2026 IJOMEST · Published under CC BY 4.0 License